

Kinematic Analysis of an Assistive Robotic Leg for Hemiplegic and Hemiparetic Patients

M.R. Safizadeh, M. Hussein, K. F. Samat, M.S. Che Kob, M.S. Yaacob, M.Z. Md Zain

Abstract—The aim of this paper is to present the kinematic analysis and mechanism design of an assistive robotic leg for hemiplegic and hemiparetic patients. In this work, the priority is to design and develop the lightweight, effective and single driver mechanism on the basis of experimental hip and knee angles' data for walking speed of 1 km/h. A mechanism of cam-follower with three links is suggested for this purpose. The kinematic analysis is carried out and analysed using commercialized MATLAB software based on the prototype's links sizes and kinematic relationships. In order to verify the kinematic analysis of the prototype, kinematic analysis data are compared with the experimental data. A good agreement between them proves that the anthropomorphic design of the lower extremity exoskeleton follows the human walking gait.

Keywords—Kinematic analysis, assistive robotic leg, lower extremity exoskeleton, cam-follower mechanism.

I. INTRODUCTION

THE third and seventh causes of death in the world are stroke and accident, respectively. In Malaysia for example, it was estimated that around 52,000 people suffer from stroke every year and six new cases occur every hour. It is considered to be the single most common cause of severe disability. On the other hand, the number of motorist involved in accident is increasing every year. Although many attempts and researches have been done to prevent the people from these events and death, the number of stroke and injured patients who survive from these events which require the rehabilitation services has been rising. The patients with hemiplegia or hemiparesis may not able to carry out the daily activities such as talking, walking, crouching and grasping; therefore, they need to improve their abilities by active and passive rehabilitation therapy iteratively and regularly. In passive exercises, the patient receive the rehabilitation exercises with physiotherapist; whereas, the active exercises are done by the patient [1].

M. R. Safizadeh is a research engineer at Intelligent Control and Automation (iCA) Lab, Faculty of Mechanical Engineering, University Teknologi Malaysia (e-mail: m.reza.safizadeh@gmail.com).

M. Hussein is the Head of Systems and Control Panel at the Faculty of Mechanical Engineering, University Teknologi Malaysia. (tel: +60 7-5534669; fax: +60 7-5566159; e-mail: mohamed@fkm.utm.my).

K. F. Samat, M.S. Che Kob are research students at Intelligent Control and Automation (iCA) Lab, Faculty of Mechanical Engineering, University Teknologi Malaysia. (email: kfadzli.samat@yahoo.com, salman_qlte@yahoo.com.my)

M.S. Yaacob is an Assoc. Professor at the Faculty of Mechanical Engineering, University Teknologi Malaysia (e-mail: shafiek@fkm.utm.my).

M.Z. Md Zain is a Senior Lecturer at the Faculty of Mechanical Engineering, University Teknologi Malaysia (e-mail: zarhamdy@fkm.utm.my).

In recent years, the attention on robotic rehabilitation has been increasing in order to train the patient base on their daily activities. However, as a reason of some, its problems such as cost, unfamiliarity of users to the device (therapists and patients) and lack of cognitive capacity to recognize and observe; the robotic rehabilitation has not been widely applied in clinics [2]. Thus, researchers have been trying to improve the interaction of robots and their environments and patients in order to carry out some beneficial repetitive exercises.

Basically, the applications and types of robots can be categorized according to the different methods of rehabilitations and can be described as follow [2]:

- (i) To train the patients with hemiplegia or hemiparesis in daily activities.
- (ii) To support and hold patients in their movement.
- (iii) To help the therapist in repetitive patients exercises.

As the number of survivors from the events such as accident, war and stroke are growing, the attention of researchers on developing robotic for lower extremity exoskeletons to help hemiplegic patients has been augmented, [3-6] and [7]. Professor Sankai in university of Tsukuba for example, has developed a hybrid assistive leg (Hal-3) which helps to improve the disable to have normal walking motion. He uses two DC motors on knee and hip joints, sensory systems in terms of rotary encoder to measure the joints angles, force sensors to measure floor reaction and myoelectricity sensor to estimate the required torques for knee and hip joints and control system [5-6]. However, since the biological signal such as myoelectricity is not estimated for HAL-3 accurately, Suzuki K. et al. proposed two new algorithms in case of floor reaction force (FRF) estimation and torso angle estimation in order to estimate patient's intentions effectively [8]. Professor Kazerooni and his research group carried out extensive research on developing Berkeley lower extremity exoskeleton (BLEEX) in order to help the people to carry significant loads in some situations such as staircases and rocky slopes, in which the wheeled vehicles are not able to accomplish these tasks. The developed system highlighted four features which include: a novel control scheme, high-powered compact power supplies, special communication protocol and electronics, and a specific architecture to decrease the complexity and power consumption [9].

Besides that, several other designs and methods of actuations have been proposed to make the patient's walking motion most comfortable. Artificial pneumatic muscles prototype; (KAFO) and (AFO) [10-14], was proposed for knee-ankle-foot orthosis and electro-pneumatic gait orthosis [15]. In addition, electrical actuators for different numbers of

DOF [5, 7, 16-17] and hydraulic actuators were also designed in order to provide the required force and torque to move the hip, knee and ankle joints correctly [9].

This paper will present the design and kinematic analysis of one DOF lower extremity exoskeleton that moves in parallel with human hip and knee joints in order to exercise the patient with repetitive and physical therapy without considering its ability to climb or walk on the stairs. A low cost, lightweight, simple and accurate mechanism is the main target of the design. It is an exoskeleton powered by a single DC motor that can synchronized the angular position and velocity of the hip and knee joints by mean of a gear and cam-follower mechanism. The cam profile is obtained base on the human motion data acquired from joint angles of the lower limbs. The necessary experiments (Fig. 1) are conducted in order to obtain the essential data (Fig. 2).

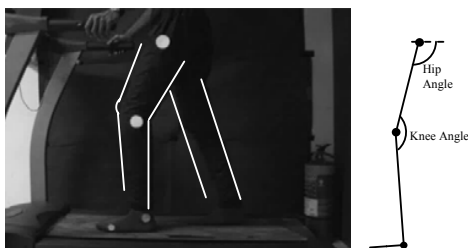


Fig. 1: Captured video in MATLAB MPlay GUI

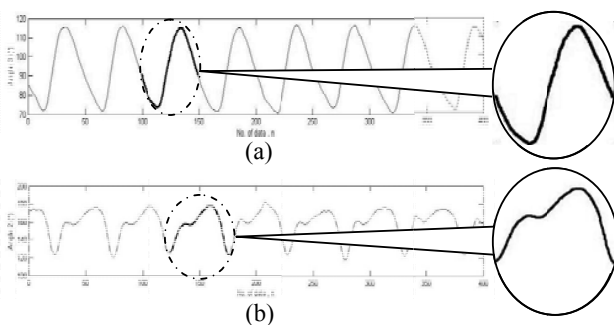


Fig. 2: Experimental Hip (a) and Knee (b) angles

II. DATA ACQUISITION AND MECHANISM DESIGN

In order to design an appropriate robotic leg, the anthropomorphic design context were followed which is divided into two major consideration. The first concern of anthropomorphic design is to make the length of each limb variable to be used for several patients. As the exoskeleton's joints should rotate in the same axis with human joint, any damage and hurt to the patient should be avoided. Another major concern is to match the leg kinematic with human motion. This is achieved through the design of a proper driver mechanism with lightweight components, less number of links and lower energy consumptions. Thus, in order to design an anthropomorphic and economic architecture, the two main links with variable length are proposed which can be fastened

to thigh and shin. To have a suitable kinematic of human motion, a mechanism consist of a DC motor, gears and cam-follower is proposed as such the knee joint motion follows the hip joint angle to make the system a single DOF mechanism as shown in Fig 3.

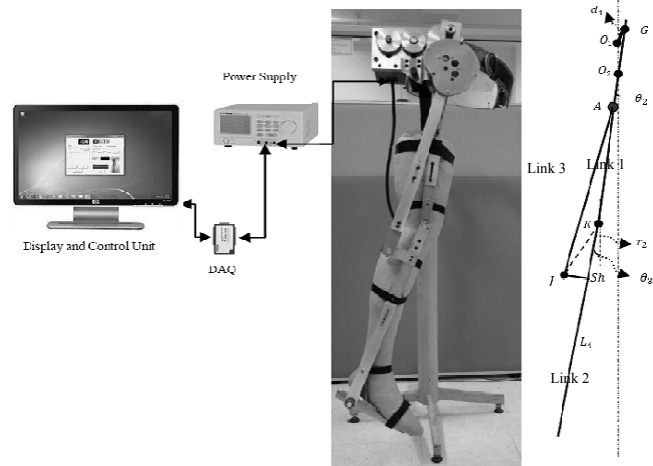


Fig. 3. Block Diagram

A. Cam Design

In the conducted experiments, human motion is captured using Sony DCR-DVD 605 with ability of 25 fps frame rate and are processed by extracting frames out of the video; thereafter. The extracted frames (Fig. 1) are processed as images using MATLAB image processing toolbox. Through image processing at the stage of data acquisition, a total 400 sequential frames are processed for walking speed of 1 km/h. The joint coordinates obtained from image processing are later used to derive joint angles and cam profile based on a single cycle data.

In the design, the hip angle is determined by gear rotation (θ_1), whereas, the knee angle depends on the link (1) motion as well as cam profile. The accuracy of cam profile therefore contributes to the accuracy of the knee angle motion. Fig. 2 illustrates that the range of angles for hip and knee movement for walking speed of 1 km/h is between 72 to 115 and 126 to 178, respectively. The angular data from both hip and knee profiles are revised to produce a more practical data thereafter before converted into follower's linear data which are used to produce the cam profile (Table 1).

III. KINEMATIC ANALYSIS

As mentioned earlier, since the powered lower limb orthosis should follow the anthropomorphic and ergonomic design, the kinematic of lower extremity exoskeleton should be proper to human motion. In order to achieve the desirable objective, the kinematic analysis of power assistive leg is carried out based on simple dynamic's relationship and MATLAB programming. The kinematic relationship of the system are acquired on the basis of kinematic analysis of three links (link

1 to 3; see Fig. 3), cam-follower and relative motion principles [18].

A. Kinematic Analysis of Link 1

Since the design and measurement of all links are obtained according to the adaption of human kinematic and lower extremity exoskeleton kinematic, link1 follows the thigh's angle with pendulous motion around point O_2 . In this design, all measurements such as d_1 and link 1 slot are acquired from patient's thigh size and the experimental data of hip angle; therefore, the size of 3.1 cm and 39.5 cm are found appropriate for d_1 and link 1, respectively as shown in Fig. 3.

In the kinematic analysis, the following assumption was made:

- The gear movement is the motion of the rod (d_1).
- Point P is a point on the slot closest to G.
- The rotating axes are assumed to be at link 1.

Based on the relative motion of rotating axes, Equation (1) to Equation (3) are introduced to formulate the velocity of one point (such as point P) on link 1.

$$V_p = V_{P/G} + V_G \quad (1)$$

$$\begin{cases} V_p - V_G \sin \theta_1 \sin \theta_2 - V_G \cos \theta_1 \cos \theta_2 = 0 \Rightarrow \\ V_p = V_G \cos(\theta_1 - \theta_2) \end{cases} \quad (2)$$

$$\begin{cases} V_{P/G} - V_G \sin \theta_2 \cos \theta_2 + V_G \sin \theta_1 \cos \theta_2 = 0 \Rightarrow \\ V_{P/G} = V_G \sin(\theta_1 - \theta_2) \end{cases} \quad (3)$$

Once the velocity of point P has been acquired, the relationship between angular velocity of link1 and angular displacement of the gear (see Fig. 5) can be obtained based on Equation (4) below.

$$\omega_2 = \theta_2 = \frac{V_p}{L_1} = \frac{V_G}{L_1} \cos(\theta_1 - \theta_2) \quad (4)$$

Where, θ_1 is the angular displacement of the gear, and L_1 and θ_2 can be expressed as follows:

$$L_1 = \sqrt{(d_1^2 + d_2^2 - 2d_1d_2 \cos \theta_1)} \quad (5)$$

$$L_1 \sin \theta_2 = d_1 \sin \theta_1 \Rightarrow \theta_2 = -\sin^{-1}\left(\frac{d_1}{L_1} \sin \theta_1\right) \quad (6)$$

Thereafter, the relationship between the absolute velocity of the knee and the angular displacement of the gear as shown in Fig. 6 is obtained from following equation:

$$V_{Knee} = L_2 \omega_2 \quad (7)$$

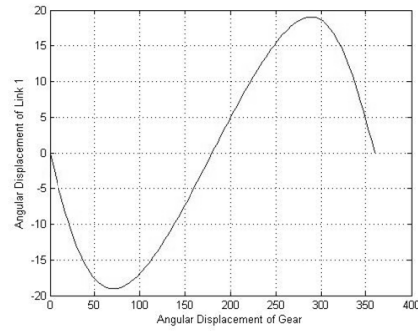


Fig. 4: Angular displacement of link 1 (θ_2)

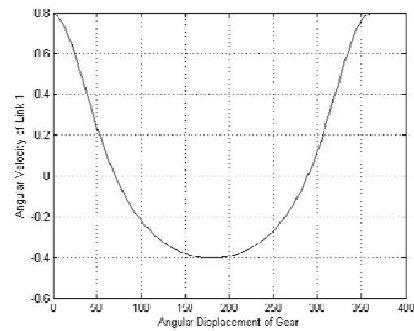


Fig.5: Angular velocity of link 1 (ω_2)

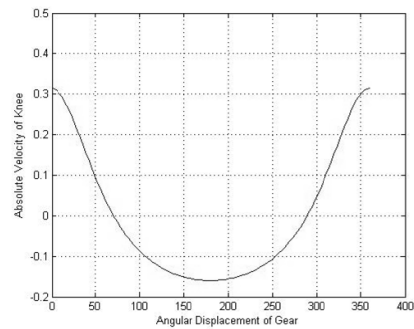


Fig.6: Absolute velocity of knee

Because of pendulous motion of link 1, the angular velocity of link 1 as well as the absolute velocity of the knee is in accordance with the pendulous motion with a frequency of 0.26 Hz. Meanwhile, the angular velocity of DC motor is 3.28 rad / s .

B. Kinematic Analysis of Link 2

In order to find the angular velocity of the link 2, the velocity of roller A; a point on follower has to be obtained. To this end, since the angular velocities for both cam and link 1 directly effected on velocity of roller, the absolute velocity of the roller can be found by dividing V_A into two velocities named, V_{A1} and V_{A2} . Velocity V_{A1} and V_{A2} are obtained by assuming the cam is rotating cam while the link is fixed and the link is rotating while the cam is fixed respectively. As

indicated earlier, the linear motion data which are used to produce cam profile are shown in Table 1. These data are represented as the graph shown in Fig. 7.

It can be seen from the graph that the displacement of the follower for rotational link is smoother than the fixed link condition in vertical direction. The profile also shows that there are dwells at the beginning and end as well as in the middle of the cycle. These are important parameters for obtaining smooth motion of the follower. Actually, this comparison is done to illustrate that the data for cam in relation with rotational link is correct and applicable. Hence it is it produces a smooth motion for the follower and the simulation.

In order to derive the kinematic relationship based on the MATLAB programming, the most correct and proper data should be acquired by interpolating the real cam profile data (Figs. 8 and Fig. 9). As the result, the absolute velocity of

roller while the link is assumed fix (V_{A1}) are demonstrated as shown in Fig.10.

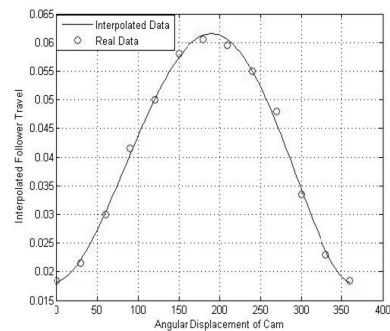


Fig. 8: Interpolated follower displacement and real data

TABLE I LINEAR MOTION DATA

| Station point Number | 0 | 1 | 2 | 33 | 4 | 5 | 6 | 7 | 8 | 9 | 10 | 11 | 12 |
|--|-------|-------|-------|-------|-------|-------|-------|-------|-------|-------|-------|-------|-------|
| Cam Angle (Deg) | 0 | 30 | 60 | 90 | 120 | 150 | 180 | 210 | 240 | 270 | 300 | 330 | 360 |
| Absolute Follower Linear Travel (Rotational Link) | 0.014 | 0.021 | 0.041 | 0.047 | 0.050 | 0.053 | 0.055 | 0.053 | 0.048 | 0.042 | 0.037 | 0.020 | 0.014 |
| Absolute Follower Linear Travel (Fixed Link) | 0.015 | 0.017 | 0.027 | 0.044 | 0.049 | 0.053 | 0.055 | 0.051 | 0.045 | 0.039 | 0.027 | 0.017 | 0.015 |

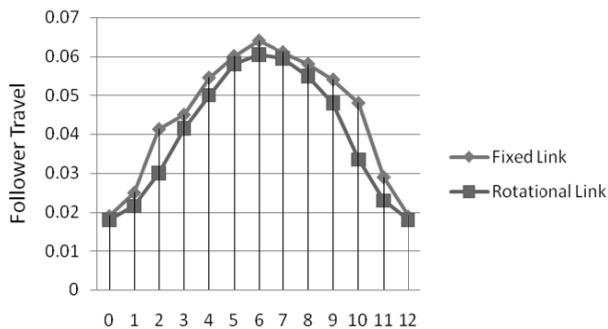


Fig.7: Cam profiles in case of fix and rotational link

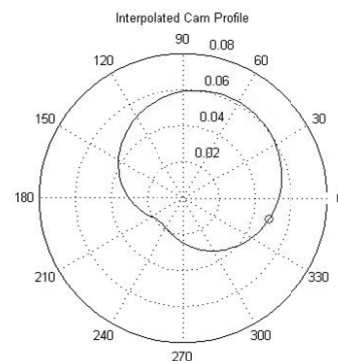
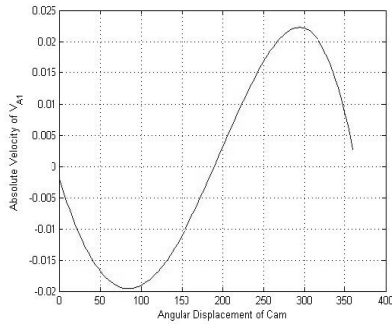
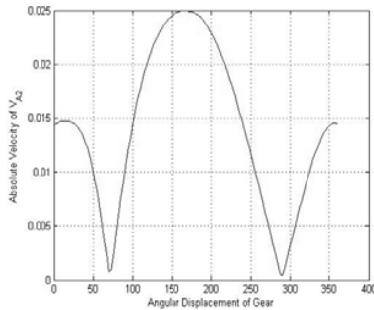
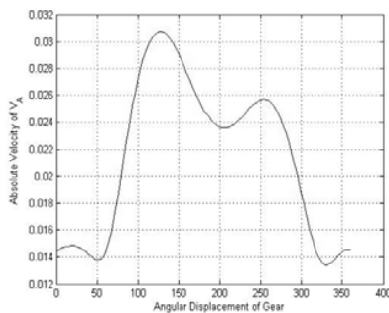


Fig. 9: Interpolated cam profile


 Fig. 10: The absolute velocity of V_{A1}

The most complicated part is to find the velocity V_{A2} . The exact position of the roller based on the rotation of the cam (θ_3) and the rod (θ_2) are needed. Subsequently, the tangential vector of cam at this position is required to calculate V_{A2} with its exact direction. Once the absolute velocity of V_{A2} is acquired (as shown in Fig. 11), by analyzing the angular velocity of link 1 and distance of roller to O_2 , and the angle between V_{A1} and V_{A2} (i.e. θ_A), the absolute velocity of the roller, V_A , is obtained based on equation (8). Fig. 12 shows the relationship between the absolute velocity V_A and the gear angular displacement.

$$V_A = \sqrt{V_{1A}^2 + V_{2A}^2 + 2V_{1A}V_{2A} \cos \theta_A} \quad (8)$$


 Fig. 11: The absolute velocity of V_{A2}

 Fig. 12: The absolute velocity of V_A

Since the lower part of exoskeleton has general motion and rotates by mean of cam-follower mechanism, the angular velocity of link 2 is acquired by utilizing the absolute velocity of roller A and the knee, and the combination of both algebraically and graphically. Consequently, the magnitude of joint Sh is generated in respect to the knee joint. On the other hand, the absolute velocity of joint J can be found by using relative motion in respect to roller A.

$$\ddot{V}_{Sh} = \ddot{V}_K + \dot{\ddot{V}}_{Sh/K} \quad (9)$$

$$\ddot{V}_J = \ddot{V}_A + \dot{\ddot{V}}_{J/A} \quad (10)$$

$$\ddot{V}_J = V_{J/Sh} + \ddot{V}_{Sh} \quad (11)$$

Since link J-Sh is fixed to link 2, the relative velocity of $V_{J/Sh}$ is zero. By equating equation (9), (10) and (11), the vector diagram shown in Fig. 13 is obtained based on equation (12) below.

$$\ddot{V}_K + \dot{\ddot{V}}_{Sh/K} = \ddot{V}_A + \dot{\ddot{V}}_{J/A} \quad (12)$$

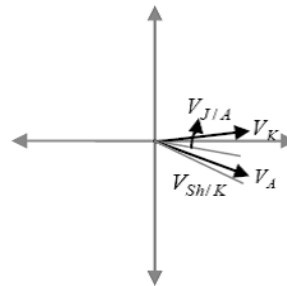


Fig. 13: Velocity vector diagram

Case I ($0 \leq \theta_1 \leq \theta_{stop_1}$)¹:

Based on the vector diagram in Fig. 13, the vector components in the x and y directions are:

$$x: V_A \sin \theta_A + V_{J/A} \cos \theta_{JA} - V_K \cos \theta_2 - V_{ShK} \cos \theta_{ShK} = 0 \quad (13)$$

$$y: -V_A \cos \theta_A - V_{J/A} \sin \theta_{JA} - V_K \sin \theta_2 + V_{ShK} \sin \theta_{ShK} = 0 \quad (14)$$

Since the magnitudes of V_K and V_A are computed from

¹ In this work the kinematic analysis of link 2 is carried out under five different conditions which are defined with respect to the angular position of link1 (θ_2). For illustration purposes only the calculations and procedures of one condition are illustrated in this paper.

equations (7) and (8), the values and direction of $V_{Sh/K}$ and $V_{J/A}$ are obtained according to equation (12) and the known angular position of link 1 (θ_2). The angular velocities of links 2 and 3 can be found by analyzing the relative velocities of $V_{Sh/K}$ and $V_{J/A}$. Once the angular velocity of link 2 is calculated, the relative velocity $V_{Bot/K}$ can be obtained using equation (15) below.

$$V_{bot/K} = \frac{L_4}{r_2} V_{Sh/K} \quad (15)$$

Since the relative velocity of $V_{Bot/K}$ can be found, the magnitude as well as the direction of ankle's velocity are obtained based on the following equations (equations (16) through (19)).

$$V_B = V_{B/K} + V_K \quad (16)$$

$$V_A = \sqrt{V_K^2 + V_{B/K}^2 + 2V_K V_{B/K} \cos(\theta_2 + \theta_{Sh/K})} \quad (17)$$

In addition, the angle between V_K and V_B is obtained, according to (18) and Fig. 14, in order to find the direction of V_B for each following case.

$$\theta_{B-K} = \cos^{-1} \left(\frac{V_B^2 + V_K^2 - V_{B/K}^2}{2 \times V_B \times V_K} \right) \quad (18)$$

$$\theta_B = -[90 - (\theta_{B-K} - |\theta_2|)] \quad (19)$$

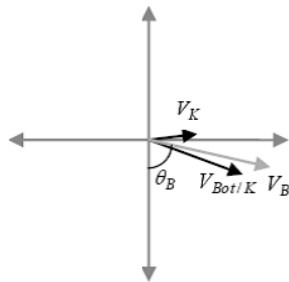


Fig. 14: Velocity vector diagram

Comparing Figs. 16 and Fig. 2(a), and Figs. 17 and Fig. 2(b), the simulation data acquired based on kinematic analysis shows good agreement with simulation results from MATLAB programming.

In order to calculate the step size for the robotic leg, it is assumed that in each step, the fore foot is vertical to the ground, and rear foot hip angle is at maximum position (17°) (see Fig. 18). Thus, the step size (d_{Step}) is calculated on the basis of known values for the link length and the hip

maximum angle.

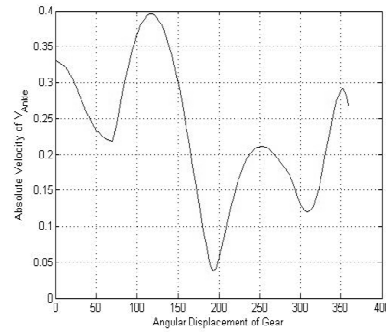


Fig. 15: Definitive absolute velocity of V_{Ankle} for one cycle

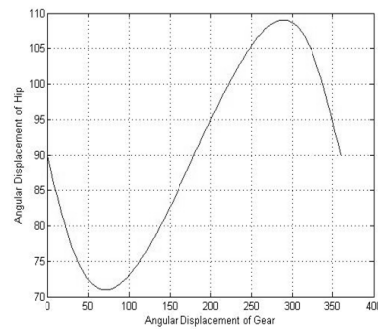


Fig. 16: Definitive angular position of hip for one cycle

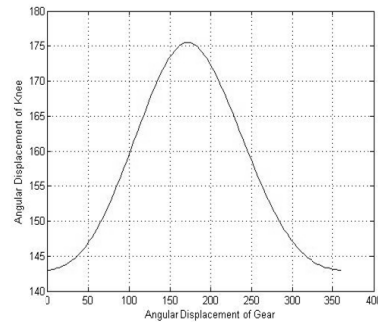


Fig. 17: Definitive angular position of knee for one cycle

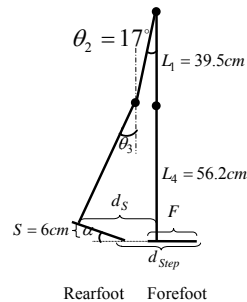


Fig. 18: Human step size during each stage of the gait

Trigonometric and geometric relationships are shown in the following equations.

$$L_1 \times \cos \theta_2 + L_4 \times \cos \theta_3 + S = L_1 + L_4 \Rightarrow \theta_3 = 24.69^\circ \quad (20)$$

$$d_S = L_1 \times \sin \theta_2 + L_4 \times \sin \theta_3 \Rightarrow d_S = 31 \text{ cm} \quad (21)$$

$$d_{Step} = d_S - F \times \sin \alpha + F \Rightarrow d_{Step} = 53 \text{ cm} \quad (22)$$

Therefore, the patient gait through a distance is $2 \times d_{Step} = 106 \text{ cm}$ in each cycle which is accordance with human step's length and within the patient's ability.

IV. CONCLUSION

This paper presents an assistive robotic leg (lower extremity exoskeleton) which was designed and developed based on acquired experimental walking data in order to help to exercise the stroke people. The experimental hip and knee angles for 1 km/h walking speed were obtained by using MATLAB image processing toolbox. Thereafter, the angular data was converted to linear motion in order to design a proper cam-follower mechanism. In this work, a significant deference between the present prototype and previous designs was the design and development of lower extremity exoskeleton mechanism using only a single DC motor to control the movement of both the hip and the knee joints. At the end, the kinematic analysis and simulation were carried out based on the proposed design. The kinematic results were compared with the experimental data to prove its validity. These validated simulation data obtained from the kinematic analysis are very useful which will be applied in our future studies.

REFERENCES

- [1] Tapus, A. & Matarić, M. J., "User Personality Matching with a Hands-Off Robot for Post-stroke Rehabilitation Therapy," in *Journal of Experimental Robotics* vol. 39, ed Heidelberg: Springer Berlin, 2008, pp. 165-175.
- [2] Moonhee, L., Matheson, R. & Hussein, A. A., "Design Issues for Therapeutic Robot Systems: Results from a Survey of Physiotherapists," *Journal of Intelligent and Robotic Systems*, vol. 42, pp. 239-252, 2005.
- [3] Kao, P.C., "Motor adaptation during dorsiflexion-assisted walking with a powered orthosis," *Journal of Gait and Posture*, vol. 29, pp. 230-236, 2009.
- [4] Sawicki, G. S., Domingo, A. & Ferris, D. P., "The Effects of Powered Ankle-Foot Orthoses on Joint Kinematics and Muscle Activation During Walking in Individuals With Incomplete spinal cord injury," *Journal of NeuroEngineering and Rehabilitation*, vol. 3, pp. 1-17, 2006.
- [5] Kawamoto, H. & Sankai, Y., "Power Assist System HAL-3 for Gait Disorder Person," in *Computers Helping People with Special Needs*. vol. 2398/2002, ed Heidelberg: Springer Berlin, 2002, pp. 19-29.
- [6] Kawainoto, H., Lee, S., Kanbe, S. & Sankai, Y., "Power Assist Method for HAL-3 Using EMG-Based Feedback Controller," in *Proceedings of the IEEE International Conference on Systems, Man, and Cybernetics*, 2003, pp. 1648-1653.
- [7] Banala, S. K., Kulpe, A. & Agrawal, S. K., "A Powered Leg Orthosis for Gait Rehabilitation of Motor-Impaired Patients," in *IEEE International Conference on Robotics and Automation*, Roma, Italy, 2007, pp. 4140-4145.
- [8] Kenta, S., Gouji, M., Hiroaki, K., Yasuhisa, H. & Yoshiyuki, S., "Intention-Based Walking Support for Paraplegia Patients with Robot Suit HAL," *Advanced Robotics*, vol. 29, pp. 1441-1469, 2007.
- [9] Zoss, A., Kazerooni & Chu, A., "On the Mechanical Design of the Berkeley Lower Extremity Exoskeleton (BLEEX)," in *IEEE/RSJ International Conference on Intelligent Robots and Systems*, 2005, pp. 3132-3139.
- [10] Ferris, D. P., Gordon, K. E., Sawicki, G. S. & Peethambaran, A., "An Improved Powered Ankle-Foot Orthosis Using Proportional Myoelectric Control," *Journal of Gait and Posture*, vol. 23, pp. 425-428, 2005.
- [11] Ferris, D. P., Sawicki, G. S. & Domingo, A., "Powered lower limb orthoses for gait rehabilitation," *Top Spinal Cord Inj Rehabil*, vol. 11, pp. 34-39, 2005.
- [12] Gordona, K. E., Sawicki, G. S. & Ferrisa, D. P., "Mechanical Performance of Artificial Pneumatic Muscles to Power an Ankle-Foot Orthosis," *Journal of Biomechanics*, vol. 39, pp. 1832-1841, 2006.
- [13] G. S. Sawicki and D. P. Ferris, "A Pneumatically Powered Knee-Ankle-Foot orthosis (KAFO) With Myoelectric Activation and Inhibition," *Journal of NeuroEngineering and Rehabilitation*, vol. 6, pp. 1-16, 2009.
- [14] Sawicki, G. S., Gordon, K. E. & Ferris, D. P., "Powered Lower Limb Orthoses: Applications in Motor Adaptation and Rehabilitation," in *9th International Conference on Rehabilitation Robotics*, Chicago, IL, USA, 2005, pp. 206-211.
- [15] Belforte, G., Gastaldi, L. & Sorli, M., "Pneumatic Active Gait Orthosis," *Journal of Mechatronics*, vol. 11, pp. 301-323, 2001.
- [16] Ruthenberg, B. J., Wasylewski, N. A. & Beard, J. E., "An Experimental Device for Investigating the Force and Power Requirements of a Powered Gait Orthosis," *Journal of Rehabilitation Research and Development*, vol. 34, pp. 203-213, 1997.
- [17] Jerry, E. P., Benjamin, T. K. & Christopher, J. M., "The Roboknee: An Exoskeleton for Enhancing Strength and Enhance During Walking," in *International Conference on Robotic & Automation*, New Orleans, 2004, pp. 2430-2435.
- [18] Meriam, J. L., Kraige, L. G. & Palm, W. J., *Engineering Mechanics: Dynamics*, 5 ed.: John Wiley, 2001.